Contribution from AT&T Bell Laboratories,
Murray Hill, New Jersey 07974

Photochromism in Dioxygen, Disulfur, and Diselenium Complexes of Rhodium and Iridium

A. P. GINSBERG,*† R. L. HARRIS, B. BATLOGG, J. H. OSBORNE, and C. R. SPRINKLE

Received April 16, 1985

$[M(X_2)(L\text{-}L)_2]^+$ (M = Rh, Ir; X_2 = chelating O_2, S_2, Se_2; L-L = dppe, dmpe) complexes are photochromic at liquid-nitrogen temperature, both in the solid state and in dilute EPA glass solution. Use of 250–350-nm light produces a color that is stable in the dark at 77 K but that is bleached back to the original color by warming to 100–110 K or by irradiation with 400–600-nm light. The photocolor is due to intense absorption in the 350–630-nm region of the spectrum. Magnetic susceptibility measurements show that photocolored $[Rh(S_2)(dmpe)_2]^+$ is diamagnetic at 10 K. SCF-Xα-SW calculations on a variety of models for the photocolored species indicate that M–X or X–X bond cleavage leads to paramagnetic ground states. Rotation of the X_2 group about the M=X_2 bond to a plane intermediate between the equatorial and axial MP_2 planes accounts for the observed spectral changes and leaves the molecule diamagnetic. The rotation can take place in an excited state where M–X_2 π bonding is weakened by occupation of an M–X_2 π^* orbital.

Introduction

Ultraviolet irradiation of the O_2 adduct of $[Ir(dppe)_2]^+$ [1] has been shown to induce reductive elimination of dioxygen and regeneration of the square-planar complex.[2] The reaction occurs in argon-purged solutions at room temperature and in EPA glasses at 77 K. In the present paper we report that UV irradiation of $[Ir(O_2)(dppe)_2]^+$, at 77 K leads to a photochromic transformation in addition to the previously reported reductive elimination. We also find that the S_2 and Se_2 analogues of the dioxygen complex, $[M(X_2)(L\text{-}L)_2]^+$ (M = Rh, Ir; X_2 = chelating S_2, Se_2; L-L = dppe, dmpe),[3] are photochromic at liquid-nitrogen temperature, but these compounds do not undergo an accompanying ultraviolet-induced reductive elimination of S_2 or Se_2. Irradiation of the solid complex, or of a dilute EPA glass solution, with 250–350-nm light produces a color that is stable in the dark at 77 K but that is bleached back to the original color by warming to 100–110 K or by irradiation with 400–600-nm light. The photocolor is due to intense absorption in the 350–630-nm region of the spectrum. Definitive characterization of the photocolored species has not been possible because of its thermal instability and the small amounts in which it is formed. We tentatively suggest that in photocolored $[M(X_2)(L\text{-}L)_2]^+$ complexes the X_2 group has rotated about the M=X_2 bond so that it lies in a plane intermediate between the equatorial and axial MP_2 planes; Xα-SW calculations on model complexes show that this accounts for the observed spectral changes. The proposed rotation can take place in an excited state where M–X_2 π bonding is weakened by occupation of an M–X_2 π^* orbital. The photobleaching process occurs at longer wavelengths than the photocoloration process because the photocolored rotamer has intense low-energy transitions to an M–X_2 π^* orbital.

Experimental Section

Irradiations were carried out with an Oriel Corp. 200-W mercury arc lamp. The light passed through a 3-in. f/0.7 UV-grade fused-silica condensing lens, an 80-mm path length circulating water filter, and one of the interference filters listed in Table I. For each interference filter, the transmitted light intensity was measured by chemical actinometry in a 1-cm quartz spectrophotometer cell positioned at the focus of the light beam.

Solutions of $[M(X_2)(L\text{-}L)_2]Cl$ complexes in EPA solvent were prepared and frozen to glasses at liquid-nitrogen temperature as previously described.[4] The cylindrical quartz Dewar in which the glass samples were prepared had an effective path length of 3.76 cm. Spectra were measured on a Cary Model 14R spectrophotometer. Temperature measurements were made with a chromel–alumel thermocouple embedded in the glass sample. Ethanol and 2-methylbutane, used for preparing EPA mixed solvent, were distilled from Linde 4A molecular sieves; diethyl ether was distilled from $LiAlH_4$. The $[M(X_2)(L\text{-}L)_2]Cl$ complexes were prepared by literature methods.[3,5]

Magnetic susceptibility measurements were made on a SQUID magnetometer built by the SHE Co. This instrument is extremely sensitive and, for our purposes, has the advantage that the sample remains stationary during changes in magnetization. The sample was a 1.0×10^{-2} M EPA solution of $[Rh(S_2)(dmpe)_2]Cl$ contained in a quartz capsule at the end of a quartz light pipe; its volume after freezing was 0.2 mL. The sample capsule and lower part of the light pipe were passed through a vacuum fitting on the magnetometer until the sample capsule was centered in the magnetometer coil. The upper part of the light pipe was positioned near the light source at a point where the entire light beam could be focused on its end. After the sample was cooled to 10 K in a 30 Oe field, it was illuminated with 303-nm light for 9 min; the change in magnetization was $<10^{-7}$ emu. Subsequent illumination with 404-nm light also resulted in a change in $M < 10^{-7}$ emu.

Table I. Interference Filter Characteristics[a]

nominal wavelength, nm	wavelength at T_{max}, nm	bandwidth at 50% of T_{max}, nm	transmitted light intens with 200-W Hg lamp, einstein/min $\times 10^6$
248	244	25	1.8
271	272	10	0.43
303	305	13	4.6
350	348	11	1.0
390	388	13	1.6
402	404	21	9.0
440	440 ± 2	14	9.6
478	478 ± 3	20	1.8
520	520 ± 4	21	0.75
560	556	16	2.1
600	600 ± 1	21	1.1

[a] Spectral characteristics of each filter were determined on a Cary Model 14R spectrophotometer.

Procedure for Calculations

SCF-Xα-SW calculations[6,7] were carried out on a Cray 1 computer as previously described[4,8] Figure 6 shows the $[Rh(S_2)(PH_3)_4]^+$ models of the photocolored complex for which the calculations were done. All bond distances and angles not explicitly noted in Figure 6 are the same as used in calculations on the normal form.[4] All calculations gave satisfactory virial ratios ($-2T/V = 1.000\,076 \pm 0.000\,023$). Slater transition states for 1-electron transitions to the virtual levels were computed in spin-restricted form.[9]

† After 1985 address correspondence to P. O. Box 986, New Providence, NJ 07974.

(1) The following abbreviations are used in this paper: ddpe, $(C_6H_5)_2PCH_2CH_2P(C_6H_5)_2$; dmpe, $(CH_3)_2PCH_2CH_2P(CH_3)_2$; EPA, 5:5:2 volume ratio of ethyl ether–isopentane–ethyl alcohol.
(2) Geoffroy, G. L.; Hammond, G. S.; Gray, H. B. *J. Am. Chem. Soc.* **1975**, *97*, 3933.
(3) Ginsberg, A. P.; Lindsell, W. E.; Sprinkle, C. R.; West, K. W.; Cohen, R. L. *Inorg. Chem.* **1982**, *21*, 3666.
(4) Ginsberg, A. P.; Osborne, J. H.; Sprinkle, C. R. *Inorg. Chem.* **1983**, *22*, 254.
(5) Vaska, L.; Catone, D. L. *J. Am. Chem. Soc.* **1966**, *88*, 5324.
(6) Slater, J. C. "The Self-Consistent Field for Molecules and Solids: Quantum Theory of Molecules and Solids"; Vol. 4, McGraw-Hill: New York, 1974; Vol. 4.
(7) Slater, J. C. "The Calculation of Molecular Orbitals"; Wiley: New York, 1979.
(8) The program used was a locally modified version of the revised Xα program package by Mike Cook, Bruce Bursten, and George Stanly.

0020-1669/85/1324-4192$01.50/0

Table II. Colors Observed on Irradiation of Powdered Crystalline Solids at Liquid-Nitrogen Temperature[a]

compd[b]	original color	irradiation wavelength,[c] nm					
		248	271	303	350	390	402
$[Rh(S_2)(dppe)_2]Cl$	m.p.	p.YG	p.YG	l.YG	l.YG	nc	nc
$[Rh(S_2)(dmpe)_2]Cl$	l.yBr	l.G	deep G	deep G	"gray"[d]	ind	ind
$[Rh(Se_2)(dmpe)_2]Cl$	brill.yG	l.yBr	l.yBr	l.yBr	l.yBr	ind	ind
$[Ir(O_2)(dppe)_2]Cl$	p.Y	l.rP	deep rP	deep rP	l.rP	ind	ind
$[Ir(S_2)(dppe)_2]Cl$	s.yPink	l.V	l.V	m.V	v.p.V	nc	nc
$[Ir(S_2)(dmpe)_2]Cl$	l.Oy	l.yBr	m.Br	m.Br	m.Br	l.yBr	l.yBr

[a] Samples were contained in 4-mm-o.d. quartz tubes immersed in liquid nitrogen in a quartz Dewar. Colors are specified by the nearest ISCC-NBS color name (supplement to NBS Circular 553): nc = no change; ind = faint color of indeterminate hue. [b] $[Ir(Se_2)(dppe)_2]Cl$ was also examined, but the color changes were to indistinct to be specified. [c] Irradiation times for the different wavelengths were such as to give the same integrated intensity, and were based on a 1.0-min irradiation with the 390-nm filter (cf. Table I). [d] Intense color of indeterminate hue.

Table III. Photobleaching of Photocolored Powders at Liquid-Nitrogen Temperature[a]

compd	photocolor[b]	irradiation wavelength,[c] nm									
		248	271	350	390	402	440	478	520	560	600
$[Rh(S_2)(dppe)_2]Cl$	l.YG	nc	nc	nc	blch	blch	blch	blch	blch	blch	blch
$[Rh(S_2)(dmpe)_2]Cl$	deep G	nc	nc	"gray"[d]	blch[e]	blch[e]	blch	blch	blch	blch	blch
$[Rh(Se_2)(dmpe)_2]Cl$	l.yBr	nc	nc	nc	blch[e]	blch[e]	blch[e]	blch[e]	blch[e]	blch[e]	blch[e]
$[Ir(O_2)(dppe)_2]Cl$	deep rP	nc	nc	nc	blch[f]	blch[f]	blch[f]	blch[f]	blch[f]	blch[f]	blch[f]
$[Ir(S_2)(dppe)_2]Cl$	m.V	nc	nc	p blch	blch[e]	blch	blch[e]	p blch	p blch	blch	blch
$[Ir(S_2)(dmpe)_2]Cl$	m.Br	nc	nc	nc	blch[e]	blch[e]	p blch	p blch	blch[e]	blch[e]	blch

[a] Samples were contained in 4-mm-o.d. quartz tubes immersed in liquid nitrogen in a quartz Dewar. The photocolor was formed by irradiation at 303 nm for 1.75 min. Abbreviations: nc, no change; blch, the photocolor is erased and the color of the unirradiated complex remains; p, partial. [b] The nearest ISCC-NBS color name. [c] Irradiations at each wavelength were timed so as to give the same integrated intensity as the color-forming irradiation at 303 nm. [d] Intense color of indeterminate hue remains. [e] A faint indication of the photocolor remains. [f] The orange color of $[Ir(dppe)_2]Cl$ remains.

Results

Irradiation of a powdered solid sample of an $[M(X_2)(L\text{-}L)_2]Cl$ complex with 250–350-nm light at liquid-nitrogen temperature causes its color to change. Table II summarizes our observations of the color changes for equal-intensity irradiations at several different wavelengths. Overall, of the wavelengths tested, 303 nm is the most effective for inducing the color change. The photocolor appears to be stable at 77 K in the dark; however, it is readily bleached by warming above liquid-nitrogen temperature or by irradiation with visible light. Thermal bleaching occurs well below room temperature and, with the exception of $[Ir(O_2)(dppe)_2]Cl$, gives back the original color of the complex. In the case of the dioxygen complex the bleached material is yellow orange in color, indicating that photodecomposition has occurred. Our observations of photobleaching of the solid samples by equal-intensity irradiations at different wavelengths are given in Table III. Bleaching occurs at all wavelengths tested from 390 to 600 nm, but all wavelengths are not equally effective. Partial bleaching was noted at 350 nm for $[Rh(S_2)(dmpe)_2]Cl$ and $[Ir(S_2)(dppe)_2]Cl$. Again with the exception of the dioxygen complex, complete photobleaching restores the color of the original complex. Photocoloration followed by photobleaching or thermal bleaching may be carried out repeatedly on the S_2 or Se_2 complexes listed in Tables II and III. However, repeated photocoloration and bleaching of $[Ir(O_2)(dppe)_2]Cl$ leads to sufficient surface decomposition after a few cycles that the photocoloration effect can no longer be seen. Figure 1 shows a spectrophotometric study of the photocoloration and photobleaching of $[Rh(S_2)(dmpe)_2]Cl$ in the solid state. The photocolored solid has new strong absorption bands at 355 and 630 nm and new shoulders at ~410 and ~260 nm. These bands are completely erased by irradiation with 402-nm light. This cycle has been repeated several times with no evidence of change in the spectra.

Preliminary experiments with dilute solutions of $[M(X_2)(L\text{-}L)_2]Cl$ complexes in EPA glasses at liquid-nitrogen temperature showed photocoloration and photobleaching similar to what was observed in the solid state. The results of a spectrophotometric study of the photochromism in EPA glasses is given in Table IV and Figures 2–4. Comparison of Figures 1 and 2 shows that the same spectral changes occur in the dilute glass as in the solid state. An estimate of the quantity of complex converted to the photocolored form in these experiments may be made from the results on $[Rh(Se_2)(dmpe)_2]Cl$. This complex has an intense band at 310 nm,[4] which after irradiation at 303 nm is observed at the same frequency with a 4% decrease in intensity. Since the new bands in the spectrum do not interfere with the 310-nm band, we conclude that about 4% of the complex has been converted to the photocolored form. For all of the compounds studied, the spectrum of the photocolored form is characterized by much more intense absorption in the low-energy region than is found in the spectrum

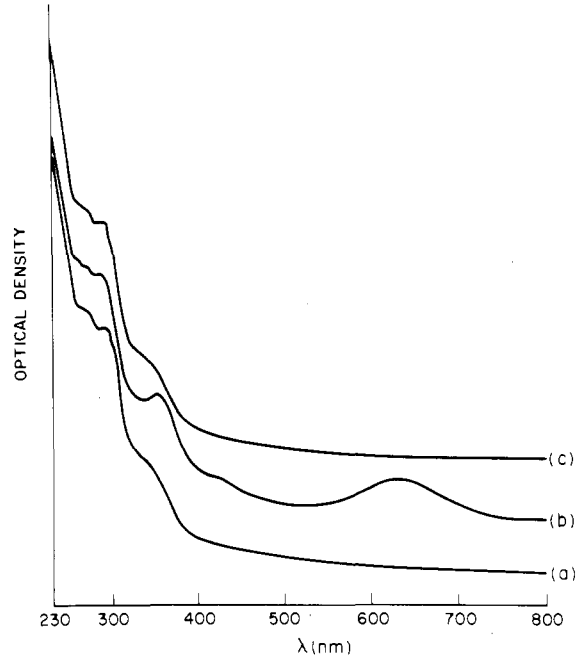

Figure 1. Photocoloration and photobleaching of $[Rh(S_2)(dmpe)_2]Cl$ in a Nujol mull at 77 K: (a) before irradiation; (b) after 2-min irradiation at 303 nm; (c) after 2-min irradiation at 303 nm followed by 2-min irradiation at 402 nm. Spectra are offset along the vertical axis for clarity.

(9) Bagus, P. S.; Bennett, B. I. *Int. J. Quantum Chem.* **1975**, *9*, 143. Ziegler, T.; Rauk, A. *Theor. Chim. Acta* **1977**, *43*, 261.
(10) Passerini, R.; Ross, I. G. *J. Sci. Instrum.* **1953**, *30*, 274.

Table IV. Electronic Absorptions for Photocolored $[M(X_2)(L\text{-}L)_2]Cl$ Complexes in EPA Glasses at Liquid-Nitrogen Temperature[a]

compd	concn,[b] M	irradiation conditions[c] time, min	irradiation conditions[c] λ, nm	λ_{max}, nm	ε, M^{-1} cm^{-1}	photobleaching at 402 nm
$[Rh(S_2)(dppe)_2]Cl$	7.56×10^{-5}	7.5	303	618	7.4×10^2	complete
				472	2.9×10^3	complete
				~440 (sh)		complete
$[Rh(S_2)(dmpe)_2]Cl$	5.36×10^{-5}	5.0	303	605	1.5×10^3	complete
				~420 (sh)		partial[d]
				355	3.6×10^3	complete
$[Rh(Se_2)(dmpe)_2]Cl$[e]	5.52×10^{-5}	4.5	303	700	6.3×10^2	complete
				~460 (sh)		complete
				~400 (sh)		complete
$[Ir(O_2)(dppe)_2]Cl$	6.12×10^{-5}	4.0	303	540		partial[f]
				430		partial[f]
$[Ir(S_2)(dppe)_2]Cl$	1.08×10^{-4}	16.0	303	540	8.8×10^2	complete
				425	9.8×10^2	complete

[a] Measurements from 300–800 nm. All of the bands listed are shifted and increased in intensity compared to nearby bands in the spectrum of the unirradiated complex; they are erased on irradiation with 402 nm light. Bands that lacked these characteristics are attributed to unconverted starting complex and are not listed in the table. [b] Corrected for solvent contraction by dividing the room temprature concentration by 0.771, the fractional change in volume of EPA on cooling from +20 to −196 °C.[10] [c] The frozen samples were contained in a cell of 3.76-cm path length. They were irradiated through a 1.0 × 2.6-cm window along the direction of the spectrophotometer beam. The incident light intensity is given in Table I. The irradiation times listed produced the maximum, or close to the maximum, absorption obtainable under these conditions. [d] A weak band due to photodecomposition remains at ~440 cm^{-1}. [e] A band at 310 nm is unshifted on irradiation; its intensity decreases by 4%. [f] After photobleaching or thermal bleaching, bands remain at 525 and 445 nm. These bands are due to square-planar $[Ir(dppe)_2]Cl$ formed by photolysis of the dioxygen complex.

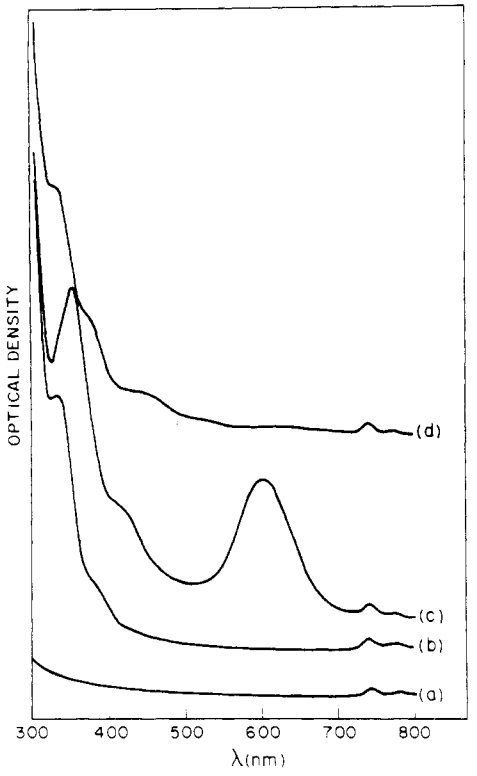

Figure 2. Photocoloration and photobleaching of 5.36×10^{-5} M $[Rh(S_2)(dmpe)_2]Cl$ in EPA glass at 77 K: (a) EPA blank; (b) before irradiation; (c) after 4-min irradiation at 303 nm; (d) after 4-min irradiation at 303 nm followed by 4-min irradiation at 402 nm. Spectra are offset along the vertical axis for clarity.

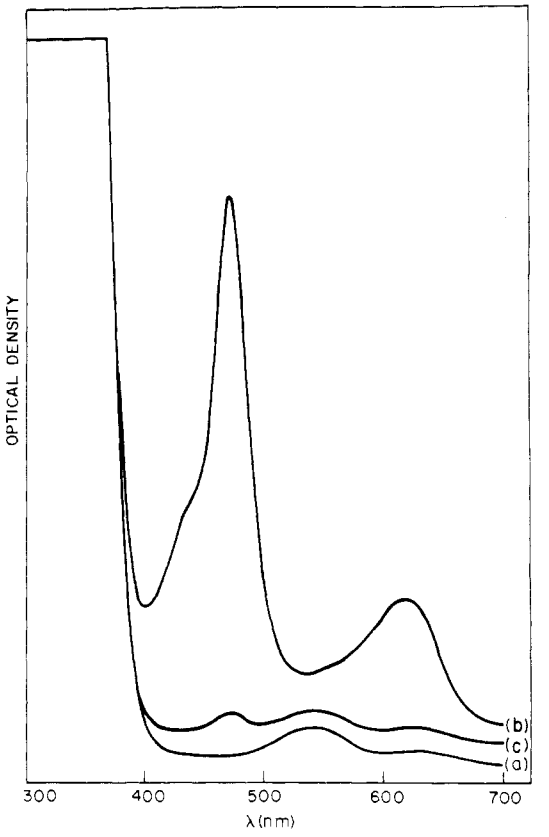

Figure 3. Photocoloration and photobleaching of 7.56×10^{-5} M $[Rh(S_2)(dppe)_2]Cl$ in EPA glass at 77 K: (a) before irradition; (b) after 4-min irradiation at 303 nm; (c) after 4-min irradiation at 303 nm followed by 4-min irradiation at 402 nm. Spectra are offset along the vertical axis for clarity.

of the normal form. Thus, normal $[Rh(Se_2)(dmpe)_2]Cl$ has bands with ε of 48 and 70 at, respectively, 617 and 708 nm[4] while after irradiation at 303 nm, the extinction at 700 nm is 6.3×10^2 (Table IV). Since only 4% of the complex was converted to the photocolored form, the actual molar extinction of the 700-nm band of photocolored $[Rh(Se_2)(dmpe)_2]Cl$ is 1.6×10^4. Assuming 5% conversion from normal to photocolored form for the other compounds in Table IV leads to an estimate of $\sim 2 \times 10^4$ for the molar extinction coefficient of the lowest energy observed band in the spectra of the photocolored forms. This is 2–3 orders of magnitude greater than ε for the nearby band in the normal complex.

Over periods of 1–2 h the spectra of the photocolored complexes in EPA glass showed no change when the sample was kept in the dark at liquid-nitrogen temperature. In the case of $[Ir(S_2)(dppe)_2]Cl$ the spectrum showed no change over an 8-h period under these conditions. Measurements of the temperature at which thermal bleaching occurred were made for $[Rh(S_2)(dmpe)_2]Cl$ and $[Ir(S_2)(dppe)_2]Cl$. With a rate of temperature rise of 1–

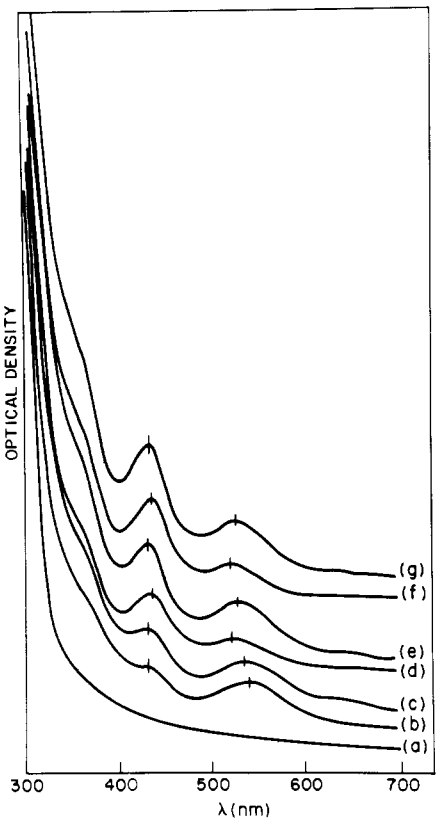

Figure 4. Repeated photocoloration and photobleaching of 6.12×10^{-5} M $[Ir(O_2)(dppe)_2]Cl$ in EPA glass at 77 K: (a) before irradiation; (b) after 2-min irradiation at 303 nm; (c) after 4-min irradiation at 303 nm; (d) after irradiation for 4 min at 303 and then 2 or 4 min at 402 nm; (e) as in spectrum d plus 4 min at 303 nm; (f) as in spectrum e plus 4 min at 402 nm; (g) as in spectrum f plus 4 min at 303 nm. Spectra are offset along the vertical axis for clarity.

2°/min., thermal bleaching of the photocolored Rh complex began at ~−173 °C while for the Ir complex bleaching did not begin until ~−160 °C; the EPA glass is still rigid at these temperatures. The spectra of $[Rh(S_2)(dppe)_2]Cl$ and $[Ir(S_2)(dppe)_2]Cl$ gave no indication of decomposition after several cycles of photocoloration followed by photobleaching, but the spectrum of $[Rh(S_2)(dmpe)_2]Cl$ in EPA glass shows evidence of slight decomposition after one cycle. As may be seen in Figure 4, $[Ir(O_2)(dppe)_2]Cl$ undergoes extensive photolysis during repeated cycles of photocoloration at 303 nm followed by photobleaching at 402 nm. Photobleaching leaves residual peaks at 525 and 444 nm, which increase in intensity after each successive cycle. These peaks are at the same wavelength as the two lowest energy absorptions of $[Ir(dppe)_2]Cl$. After each 303-nm irradiation the 525-nm peak shifts to longer wavelength and the 444-nm peak shifts to shorter wavelength due to formation of the photocolored form of $[Ir(O_2)(dppe)_2]Cl$. The shift decreases with each successive cycle as photodecomposition product accumulates and photocoloration decreases.[11]

Figure 5 shows the results of some rate measurements on the photocoloration and photobleaching of $[Rh(S_2)(dmpe)_2]Cl$ in EPA glass. From the lower part of the figure it is evident that neither process follows a first-order rate law. The upper part of the figure indicates that $dA/dt \propto 1/t$, where A is the absorbance of the

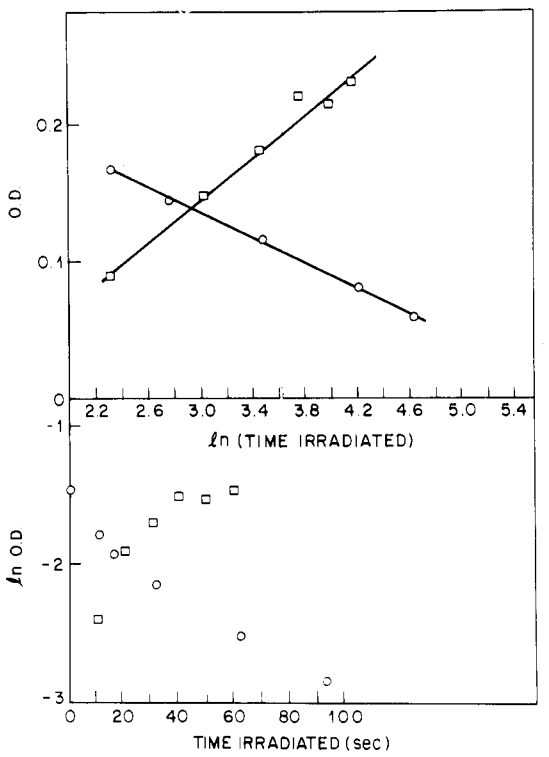

Figure 5. Rate of photocoloration and photobleaching of $[Rh(S_2)(dmpe)_2]Cl$ in EPA glass at 77 K: (□) absorbance and ln (absorbance) at 605 nm as a function of irradiation time at 303 nm; (○) absorbance and ln (absorbance) of the photocolored complex at 605 nm as a function of bleaching with 404-nm radiation.

photocolored form after irradiation time t for irradiation at either 303 or 402 nm. In view of the conditions of the experiment (rigid medium) and the fact that the photocolored form absorbs strongly at 303 nm, failure to follow a first-order rate law has no mechanistic significance.

If the photocolored species is paramagnetic it would be expected to have $S = 1$. With the assumption that $g = 2.0$, the observed upper limit (10^{-7} emu) for the change in magnetization on irradiation with 303-nm light corresponds to the formation of $<1.9 \times 10^{13}$ paramagnetic centers. This in turn means that, if we make the very conservative assumption that the concentration of photocolored complex in the sample was 2.0×10^{-6} M,[12] <8% of the photocolored molecules can be in an $S = 1$ state. We therefore conclude that the photocolored complex is diamagnetic.

Discussion

We have established that $[M(X_2)(L\text{-}L)_2]^+$ complexes undergo a photochromic change in dilute glass solution at 77 K and that the photocolored form is stable for relatively long periods of time (at least several hours). From these facts it is clear that the photocoloration is not a solid-state effect, nor is it simply due to an excited electronic state of the normal complex. The photocolor must result from a change in the bonding of the normal form of the complex ion. In this discussion we will use what is known about the electronic structure of the complexes in their normal state,[4] together with the results of new $X\alpha$–SW calculations on $[Rh(S_2)(PH_3)_4]^+$ in several different bonding configurations, to speculate about the probable nature of the photocolored complexes.

Table V lists the highest and next to highest energy absorption bands tht have been reported for normal $[M(X_2)(L\text{-}L)_2]^+$ (X_2 = S_2, Se_2) complexes at 77 K. The assignments for the bands based on $X\alpha$–SW calculations are also given in the table. Comparison

(11) A 20-min irradiation of a 6.12×10^{-5} M solution of $[Ir(O_2)(dppe)_2]Cl$ in EPA glass at 77 K with 350-nm light produced only very faint absorption in the 400–600-nm region. This is consistent with the report[2] that no color change was observed when an EPA glass containing the dioxygen complex was irradiated at liquid-nitrogen temperature with 366-nm light. However, the proposal[2] that photolysis actually took place but that the color of the square-planar complex is not seen because the rigid glass prevents the phosphine ligands from rearranging to the square-planar geometry is inconsistent with our observation of the square-planar absorption bands after irradiation with 303-nm light.

(12) The irradiated sample in the magnetic susceptibility measurements was more intensely colored than in the spectrophotometric studies. Since in the latter experiments the concentration of photocolored form was ca. 2.0×10^{-6} M, this value is a lower limit for the concentration in the magnetic susceptibility sample.

Table V. Highest and Next to Highest Energy Absorption Bands in Normal $[M(X_2)(L\text{-}L)_2]^+$ Complexes[a]

complex	λ_{max}, nm	ϵ, M^{-1} cm^{-1}	assignt
$[Rh(S_2)(dppe)_2]^+$	306	2.6×10^4	$10a_1 \rightarrow 7b_1$ ($^1B_1$)
			$6b_1 \rightarrow 11a_1$ ($^1B_1$)
			$4a_2 \rightarrow 8b_1$ ($^1B_2$)
	345	1.0×10^4	$6b_1 \rightarrow 7b_1$ ($^1A_1$)
$[Rh(S_2)(dmpe)_2]^+$	288	2.5×10^4	$10a_1 \rightarrow 7b_1$ ($^1B_1$)
			$6b_1 \rightarrow 11a_1$ ($^1B_1$)
			$4a_2 \rightarrow 8b_1$ ($^1B_2$)
	330		$6b_1 \rightarrow 7b_1$ ($^1A_1$)
$[Rh(Se_2)(dmpe)_2]^+$	310	1.2×10^4	$10a_1 \rightarrow 7b_1$ ($^1B_1$)
			$6b_1 \rightarrow 11a_1$ ($^1B_1$)
			$4a_2 \rightarrow 8b_1$ ($^1B_2$)
	389	7.2×10^2	$6b_1 \rightarrow 7b_1$ ($^1A_1$)
$[Ir(S_2)(dppe)_2]^+$	310	7.8×10^3	$10a_1 \rightarrow 7b_1$ ($^1B_1$)
			$4a_2 \rightarrow 8b_1$ ($^1B_2$)
			$6b_1 \rightarrow 7b_1$ ($^1A_1$)
	~340		$6b_1 \rightarrow 7b_1$ ($^3A_1$)
			$10a_1 \rightarrow 7b_1$ ($^3B_1$)

[a] From ref 7 except for $[Rh(S_2)(dmpe)_2]^+$, which was not reported previously.

of Table V with the results in Tables II and III indicates that the strong 306–310-nm (288 nm in $[Rh(S)_2(dmpe)_2]^+$) absorption is responsible for the photochromic effect. The longer wavelength absorption listed for each complex in Table V also appears to cause photocoloration, but in some cases it is less active, either because it is a weaker absorption or because it falls close to an intense bleaching absorption of the photocolored form. We may assess the possible bonding changes in the excited states produced in these absorptions by examining the nature of the orbitals involved in the transitions. Transition $6b_1 \rightarrow 11a_1$ ($^1B_1$) is omitted since it is not a candidate transition for $[Ir(S_2)(dppe)_2]^+$. The originating orbitals are $10a_1$, $6b_1$, and $4a_2$; $6b_1$ is M–X_2 π and X–X π^*, $4a_2$ is X–X π^*, and in $10a_1$ the interactions are weak. The terminating orbitals are $7b_1$ and $8b_1$; $7b_1$ is M–X_2 π^* and X–X π^*, and $8b_1$ is X–X σ^*. In the $10a_1 \rightarrow 7b_1$ ($^1B_1$) excited state the M–X and the X–X π interactions will be weakened. In the $4a_2 \rightarrow 8b_1$ ($^1B_2$) excited state the X–X σ bond will be weakened, although this is partly compensated by increased X–X π interaction. In the $6b_1 \rightarrow 7b_1$ ($^1A_1$) excited state the major effect will be decreased M–X_2 π bonding. To this list of excited states we also add the lowest energy excited states $4a_2 \rightarrow 7b_1$ ($^1B_2$ or $^3B_2$), which can be reached by decay of one of the previous more highly excited states;[13] this state is characterized by weakened M–X_2 π interaction. The most likely bonding changes in these excited states are therefore rupture of the X–X bond, rupture of an M–X bond,[14] and rotation of the X_2 group about the M–X_2 bond; the latter could occur in a state where the M–X_2 π interaction is weakened, leading to a decrease in the barrier to rotation about the bond.[15]

In view of the preceeding analysis we considered the bonding configurations shown in Figure 6 as models for the photocolored complexes. For each of these models the ground state electronic structure was calculated by the SCF–Xα–SW method; Figure 7 is a diagram of the results.

Model 1. An Rh–S bond has broken, and the S_2 group remains bonded to rhodium in the supersulfide configuration. The Xα–SW calculation predicts a paramagnetic ($S = 1$) ground state for this model, in disagreement with the observed diamagnetism of the photocolored complex.

Model 2. The S–S bond has broken, and the S atoms have separated to a noninteracting distance. Again the calculations given an $S = 1$ ground state in disagreement with experiment.

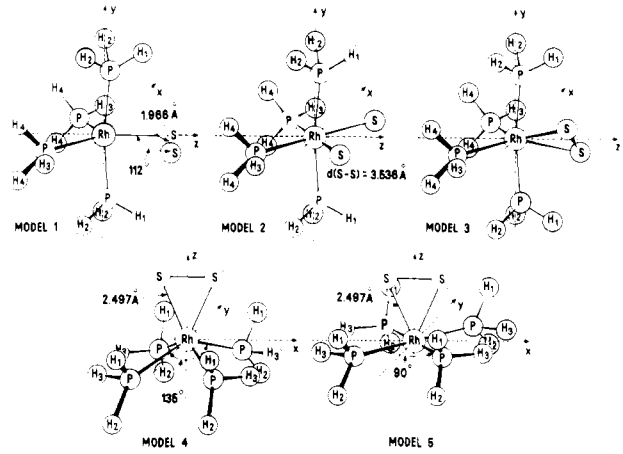

Figure 6. $[Rh(S_2)(PH_3)_4]^+$ models of the photocolored complex for which SCF–Xα–SW calculations were carried out. Unless otherwise indicated bond distances and angles were the same as in the normal form:[4] model 1, supersulfide structure, C_s symmetry; model 2 S–S bond broken and S atoms separated, C_{2v} symmetry; model 3, S_2 group rotated 45° clockwise about Rh–S_2 bond (z axis), C_2 symmetry (in model 3a the S_2 is rotated and the Rh–S distance is 0.1 Å longer than in the normal form); model 4, S_2 group as in model 3a and PH_3 groups at base of a square pyramid with Rh at its apex, C_{2v} symmetry; model 5, S_2 group as in model 3a and PH_3 groups coplanar with Rh, C_{2v} symmetry.

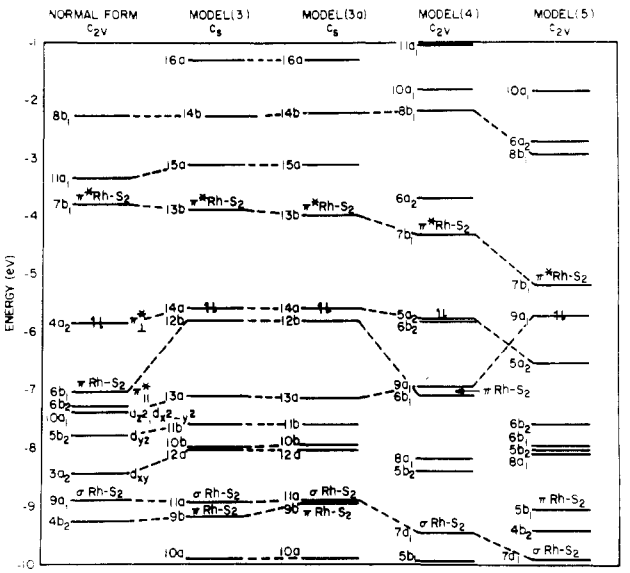

Figure 7. Upper valence energy levels of the normal form[4] of $[Rh(S_2)(PH_3)_4]^+$ and of several models for the photocolored form as calculated by the SCF–Xα–SW method. Dashed lines connect related orbitals with similar charge distributions but not necessarily the same bonding character.[16]

Model 3. The S_2 group has rotated 45° about the Rh–S_2 bond. This causes the strong in-plane π-Rh–S_2 interaction in level $6b_1$ of the normal form to completely disappear in the corresponding level 12b of model 3. However the out-of-plane π-Rh–S_2 interaction of normal-form level $4b_2$ is enhanced in model 3 level 9b; there are no occupied antibonding levels in model 3 to cancel this interaction (unlike the normal form where the out-of-plane π bond is largely canceled by a π^* interaction in level $6b_2$). The major antibonding π-Rh–S_2 interaction in model 3 occurs in the LUMO, level 13b, between an Rh d_{xz},d_{yz} hydrid and an S_2 π^* orbital. Overall, rotation of the S_2 group by 45° has caused the Rh–S_2 π bond in model 3 to be weaker than in the normal form. In model 3a the Rh–S_2 distance has been increased by 0.1 Å, with the result that there is a small increase in the energy of Rh–S_2 bonding levels and a small decrease in energy of Rh–S_2 antibonding levels.

Model 4. The S_2 group remains as in model 3a, but the equatorial P–Rh–P angle has been opened to 135° and the axial angle has been reduced to 135° to put the PH_3 groups at the base

(13) All of the complexes fluoresce on photocoloration by irradiation with 303-nm light.
(14) We do not consider the possibility of rupture of both M–X bonds, i.e. photodissociation of the X_2 group, since, in the absence of irreversible photolysis, the spectra of the photocolored compounds show no evidence of $[M(L\text{-}L)_2]^+$ complexes.
(15) In the normal form these compounds have only in-plane M–X_2 π bonding.
(16) Bonding character was determined from wave function contour maps.

Table VI. Dipole-Allowed Transitions below 4.0 eV for Model 3a

transition	description[a]	predicted intens[b]	calcd energy,[c] eV	obsd energy, eV: photocolored $[Rh(S_2)(dppe)_2]Cl$	obsd energy, eV: photocolored $[Rh(S_2)(dmpe)_2]Cl$
14a → 13b	$\pi_\perp^* \rightarrow \pi_\parallel^*, d_{in}$	w	1.70	*d*	*d*
12b → 13b	$\pi_\parallel^* \rightarrow \pi_\parallel^*, d_{in}$	s	1.84	2.01	2.05
12b → 15a	$\pi_\parallel^* \rightarrow d_\parallel; \pi_\perp^* \rightarrow d_{out}$	s	2.71	2.63	2.95
14a → 15a	$\pi_\perp^* \rightarrow d_{out}$	s	2.81	2.82	
13a → 13b	$d_\parallel \rightarrow \pi_\parallel^*$	s	3.21	*e*	3.49
14a → 14b	$\pi_\perp^* \rightarrow p\sigma^*$	w	3.31	*d, e*	*d*
12b → 14b	$\pi_\parallel^*, d_\perp \rightarrow p\sigma^*$	w	3.71	*d, e*	*d*
11b → 13b	$P_{ax}, d_{yz} \rightarrow \pi_\parallel^*, d_{out}$	w	3.80	*d, e*	*d*

[a] Important components contributing to the transition. σ and π are the S_2 basis functions; an asterisk designates an antibonding combination, while subscripts $\parallel$ and $\perp$ indicate respectively that the orbital has its nodal plane perpendicular and parallel to the Rh–S_2 plane. d_{in} and d_{out} are Rh atom d orbitals with large components in, respectively, the Rh–S_2 plane and the plane through an Rh–S bond and perpendicular to the Rh S_2 plane. [b] Transitions are classified as s (strong) or w (weak) on the basis of the orbital description shown in the second column: Transitions are called strong if they contain an M → L or L → M charge-transfer component between orbitals with large fractions of their charge density in the same plane; they are also called strong if there is an intraligand component transition between orbitals with coincident charge density. If all of the significant transition components are between orbitals having most of their charge density in orthogonal planes, the transition is called weak. d–d transitions are taken to make a weak contribution to the intensity. [c] Spin-restricted transition-state calculations. [d] Under the conditions of our experiment, with ~5% conversion to the photocolored form in a solution $\sim 5 \times 10^{-5}$ M in the normal complex, a weak band would probably not be observed. [e] Under the conditions of our experiment, absorption maxima above ca. 3.4 eV would not have been observed in photocolored $[Rh(S_2)(dppe)_2]Cl$.

Table VII. Dipole-Allowed Transitions below 4.0 eV for Model 4 (Footnotes As in Table VI)

transition	description[a]	predicted intens[b]	calcd energy,[c] eV	obsd energy, eV: photocolored $[Rh(S_2)(dppe)_2]Cl$	obsd energy, eV: photocolored $[Rh(S_2)(dmpe)_2]Cl$
$5a_2 \rightarrow 7b_1$	$\pi_\perp^* \rightarrow \pi_\parallel^*, d_{xz}$	w	1.64	*d*	*d*
$6b_2 \rightarrow 6a_2$	Rh → P in P–Rh–P plane	s	2.19	2.01	2.05
$9a_1 \rightarrow 7b_1$	$dz^2, d_{x^2-y^2} \rightarrow \pi_\parallel^*, d_{xz}$	s	2.69	2.63	
$5a_2 \rightarrow 6a_2$	$\pi_\perp^* \rightarrow$ P, Rh in P–Rh–P plane	w	2.78	*d*	2.95
$6b_1 \rightarrow 7b_1$	$\pi_\parallel^* \rightarrow \pi_\parallel^*, d_{xz}$	s	2.82	2.82	
$6b_1 \rightarrow 6a_2$	Rh → P in P–Rh–P plane	s	3.57	*e*	3.49
$5a_2 \rightarrow 8b_1$	$\pi_\perp^* \rightarrow p\sigma^*$	w	3.61	*d, e*	*d*

Table VIII. Dipole-Allowed Transitions below 4.0 eV for Model 5 (Footnotes As in Table VI)

transition	description[a]	predicted intens[b]	calcd energy,[c] eV	obsd energy, eV: photocolored $[Rh(S_2)(dppe)_2]Cl$	obsd energy, eV: photocolored $[Rh(S_2)(dmpe)_2]Cl$
$9a_1 \rightarrow 7b_1$	$d_{z^2} \rightarrow \pi_\parallel^*, d_{xz}$	s	0.73	2.01	2.05
$5a_2 \rightarrow 7b_1$	$\pi_\perp^* \rightarrow \pi_\parallel^*, d_{xz}$	w	1.44	*d*	*d*
$9a_1 \rightarrow 8b_1$	$d_{z^2} \rightarrow p\sigma^*$	s	3.17	2.63	
					2.95
$6b_1 \rightarrow 7b_1$	$d_{xz} \rightarrow \pi_\parallel^*, d_{xz}$	s	3.20	2.82	
$8a_1 \rightarrow 7b_1$	$d_{x^2-y^2} \rightarrow \pi_\parallel^*, d_{xz}$	s	3.43	*e*	3.49
$5a_2 \rightarrow 8b_1$	$\pi_\perp^* \rightarrow p\sigma^*$	w	3.61	*d, e*	*d*

of a square pyramid with Rh at its apex. π-Rh–S_2 interaction in this model occurs in level $6b_1$; it is of the in-plane type, very similar to but slightly weaker than what is found in the normal form.

Model 5. Again the S_2 group remains as in model 3a, but now the PH_3 ligands have been made coplanar with the Rh atom. Contour maps show the π-Rh–S_2 and π^*-Rh–S_2 interactions in this model to be essentially the same as in model 4 and as in the normal form.

The results of the Xα–SW calculations indicate that the hypothesis of photocoloration by rupture of an Rh–S or S–S bond is inconsistent with the magnetic susceptibility measurements. We are left with the hypothesis of photocolortion by rotation of the S_2 group out of the metal–phosphine ligand plane. The Xα calculations show that a 45° rotation of the S_2 group causes the Rh–S_2 π interaction to become weaker and to shift from an in-plane to an out-of-plane bond.[17] A 45° rotation together with rearrangement of the PH_3 ligands as in models 4 or 5 leads to retention of the normal-form in-plane π interaction.

Tables VI, VII, and VIII give the calculated spin-restricted Slater transition-state energies and estimated intensities for the dipole-allowed transitions with energies below 4.0 eV for models 3a, 4, and 5. Comparison with the observed absorptions for photocolored $[Rh(S_2)(dppe)_2]^+$ and $[Rh(S_2)(dmpe)_2]^+$ shows that models 3a and 4 are in reasonably good agreement with experiment while the agreement with model 5 is poor. The Xα calculations therefore show that a 45° rotation of the S_2 group, either with or without accompanying rearrangement of the phosphine ligands as in model 4, causes the spectrum of $[Rh(S_2)(PH_3)_4]^+$ to change in the way observed when $[Rh(S_2)(dppe)_2]^+$ or $[Rh(S_2)(dmpe)_2]^+$ are photocolored: intense transitions, which in the normal form of the complex occur above 3.5 eV, are shifted down to the 2.0–3.5-eV region. We conclude that the hypothesis of X_2 group rotation accounts for the information presently available on photocoloration of $[M(X_2)(L\text{-}L)_2]^+$ complexes. Photobleaching of the photocolored rotamer can occur when the barrier to rotation is reduced by exciting an electron into the π^* M–X_2 LUMO of the rotamer. Long-wavelength light (~600 nm) is effective in doing this since it is intensely absorbed by the HOMO → LUMO transition and is well removed from the wavelengths that cause photocoloration of the normal complex.

(17) On further rotation to 90°, the π bond remains out-of-plane and the strength of the interaction, as judged from contour plots, remains about the same.

Registry No. $[Rh(S_2)(dppe)_2]Cl$, 82522-19-8; $[Rh(S_2)(dmpe)_2]Cl$, 82522-20-1; $[Rh(Se_2)(dmpe)_2]Cl$, 82522-23-4; $[Ir(O_2)(dppe)_2]Cl$, 29894-56-2; $[Ir(S_2)(dppe)_2]Cl$, 47898-17-9; $[Ir(S_2)(dmpe)_2]Cl$, 82522-18-7; $[Rh(S_2)(PH_3)_4]^+$, 83632-71-7.